Chapter 3

Power-Adaptive Decode-and-Forward Relaying Policy

The previous chapter presented a simple and intuitive PRSP for a cooperative D2D communication system. Further it was also discussed that a relay selection policy with an optimized relaying policy can significantly enhance the performance of the cooperative D2D communication system model. Therefore, in this chapter, we propose a PA-DAF relaying policy. In this chapter, we first discuss the system model and the transmission protocol in Section 3.1. Section 3.2 defines the optimization problem for each performance measure and presents optimized results for each of them based on the optimized relay gain. Further, in Section 3.3, we present the numerical results for the proposed optimal performance measures and compare them with benchmark policies. Lastly, in Section 3.4, we provide a summary of the work done in this chapter. The proof of all the results is relegated in Appendix B.

3.1 System Model and Transmission Protocol

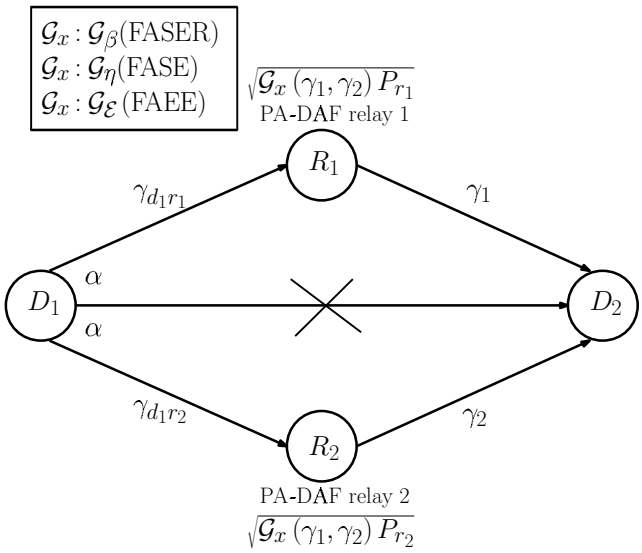

Figure 3.1: PA-DAF relay-assisted, D2D cooperative wireless communication system.

Figure 3.1 illustrates our cooperative D2D wireless system model. For this four node system, we assume that destination node D_2 is not in the transmission range of source node D_1 [97]. Therefore, reliable communication between D_1 node and D_2 node is not possible. Two relay nodes are available, and they help in forwarding source information. To reliably transfer data symbol, denoted by α, from D_1 node to D_2 node, either the relay node R_1 or the relay node R_2 is used. The selection of the relay node that forwards its received signal is based on the PRSP, which was described in chapter 2.

In the four node system, we assume that each node has a single transmitting or receiving RF antenna [98]. The relay nodes are half-duplex, and all transmissions occur over the same bandwidth [96]. All the wireless channels are assumed to be Rayleigh frequency-flat fading channels and are statistically independent of each other [99]. We assume that the selected relay node acquires the required CSI [56, 104]. The knowledge of CSI is essential because the selected relay has to optimally adapt its key parameters like gain and transmit power as a function of channel gains of the links between itself to the destination device. Therefore, these relays are called PA-DAF relays.

Remarks on power adaptation: The proposed cooperative D2D system consists of average power-constrained, PA-DAF relays. The selected PA-DAF relay optimally sets the gain and power to optimize end performance measures, namely, FASER, FASE, and FAEE. Therefore, the optimal policies that we derived are power adaptation policies.

Note that only the relay transmit power is constrained for the proposed PRSP with PA-DAF relaying. There is no total power constraint or source power constraint. The source node's transmit power is fixed and not constrained. We assume that the destination node is not in the reliable transmission range of source for the proposed system models. Therefore, the received signal at the destination node is due to the relay node transmissions based on the proposed relaying policy.

Furthermore, the PRSP policy selects the relay based on weights, which are the functions of the first hop's average SNRs. Therefore, the signal received at the destination is the sum of all the signals received from the two relays weighted by their corresponding probabilities.

Remarks on impact of existence of direct link on the system model: Note that the destination node receives the signal only from the selected relay. If a reliable direct link exists, combining techniques like maximal ratio combining (MRC) or selection combining can be employed at the destination. It is important to note that employing MRC at the destination will increase the performance of the system model, however,

at the cost of increased complexity at the destination node. The analysis presented can be extended easily to a cooperative system model having MRC at the destination.

Below, we present remarks on the usefulness of the proposed model in a cooperative multi-hop network perspective.

3.1.1 Comments on the Usefulness of the Model

One can view the proposed four-node model as a diamond lattice for a large scale multi-hop cooperative D2D network consisting of several relay nodes [105]. The usefulness of the proposed model is as follows. Suppose that a source node has to deliver a packet to a destination node via intermediate PA-DAF relay nodes. For it, an optimal route from source to destination can be determined based on the PRSP and optimal relaying policies to deliver the packet in a more reliable or spectrally efficient or energy efficient manner. However, note that deriving the optimal policies for the proposed model are non-trivial and challenging.

3.1.2 Transmission Protocol for System Model

Consider transmission of information symbol α having unit energy. The cooperative D2D transmission protocol occurs in two time slots, as described in Table 3.1. Note that the data symbol α belongs to MPSK or MQAM constellations. We assume that the data symbols are equally likely. P_{d_1}, and P_{r_i} respectively, denote the transmit power of D_1 node, and R_i ($i = 1$ or $i = 2$) nodes. Furthermore, the channel fading coefficient of D_1–R_i link (that is $h_{d_1 r_i}$), and R_i–D_2 link (that is $h_{r_i d_2}$) are $\mathcal{CN}(0, \delta^2_{d_1 r_i})$, and $\mathcal{CN}(0, \delta^2_{r_i d_2})$, respectively, and $n_{d_1 r_i}$ and $n_{r_i d_2}$ denotes additive white Gaussian noise (AWGN) components at R_i and D_2 respectively, which are independent of each other and to channel gains.

Relay characterization and design: In the cooperative D2D transmission protocol described in the table, the value of i ($i = 1$ or $i = 2$) depends on the selected relay based on the PRSP. Unlike the conventional DAF relays, we consider power constrained, power-adaptive DAF relays in our cooperative D2D system model. The PA-DAF relay's average transmit power is constrained to a threshold power. Before transmitting its signals to the destination, the selected PA-DAF relay sets optimal relay gain and transmit power (while satisfying the constraint) based on the channel power gain of the link between itself to the destination node. We name this amplification as an optimal relay gain function (RGF). We represent optimal RGF mathematically by $\mathcal{G}^*_x(\gamma_1, \gamma_2)$, where γ_1, and γ_2, are instantaneous channel power gain of $R_1 - D_2$ link, and $R_2 - D_2$ link, respectively. Below, we compare functional differ-

Table 3.1: Transmission protocol for the cooperative D2D system with PA-DAF relays. Relay selection policy selects the relay i ($i = 1$ or $i = 2$.).

Time Slot	Transmit Node	Receive Node	Received Signal Expression
Slot 1	D_1	R_i	$y_{d_1 r_i} = \sqrt{\tilde{P}_{d_1}} h_{d_1 r_i} \alpha + n_{d_1 r_i}$, where $\tilde{P}_{d_1}$ is relay received power.
Slot 2	R_i	D_2	$y_{r_i d_2} = \sqrt{\mathcal{G}_x(\gamma_1, \gamma_2)\, \tilde{P}_{r_i}} h_{r_i d_2} \alpha + n_{r_i d_2}$, where $\tilde{P}_{r_i}$ is D_2 received power, $\mathcal{G}_x(\gamma_1, \gamma_2)$ is relay gain function and $x = \beta$ (for FASER), η (for FASE) and, $\mathcal{E}$ (for FAEE).

ences between (i) AAF relay versus PA-DAF relay and (ii) DAF relay versus PA-DAF relay.

AAF relay versus PA-DAF relay: AAF relay is one of the widely used relays, given its simplicity and ease of implementation. It is a non-regenerative relay, with the main task to amplify the received signal and transmit it to the destination. The main drawback of this relay is its noise amplification. On the other hand, PA-DAF relay has more tasks to perform and so is more complicated. In it, the signal received is first decoded and re-encoded. Later, the re-encoded signal is amplified optimally based on the channel conditions. PA-DAF relay improves the end SNR of the signal received at the destination in comparison to AAF relay scenario. Furthermore, the CSI required for the fixed gain or fixed power AAF relay to forward the signal to the destination is negligible. On the other hand, for PA-DAF relay, instantaneous CSI between the relays to destination links are required to evaluate the RGF to amplify the re-encoded signal optimally.

DAF relay versus PA-DAF relay: DAF relay is also regenerative relay, whose tasks are to decode and re-encode the received signal and then forward the signal to the destination. The primary difference between the DAF relay and PA-DAF relay is that the PA-DAF relay apart from working as a conventional DAF relay, it also amplifies the received signal optimally, depending on the channel conditions. This amplification is based on RGF $\mathcal{G}(\gamma_1, \gamma_2)$ and is a function of γ_1, and γ_2, which are channel power gain of $R_1 - D_2$ link, and $R_2 - D_2$ link, respectively.

3.1.3 Remarks on PA-DAF Relay Complexity

The implementation complexity is high for PA-DAF relay when compared to the conventional AAF relay and DAF relay. However, for specific applications such as cooper-

ative D2D multihop networks where we need to optimize the PHY layer performance measures, namely, FASER, FASE and FAEE, such optimal relaying policies are essential. Furthermore, considering conventional relays, AAF, or non-regenerative fixed gain relays have negligible processing complexity because of their non-regenerative nature.

On the other hand, DAF relays have considerable decoding complexity. However, due to the development of low complexity decoders [106] and fast and efficient computing processors, the decoder complexity of DAF relay can be significantly reduced. In the proposed system model, PA-DAF relay's complexity includes the decoder complexity and computational time complexity involved in computing the optimum relay gain function. However, the problem of computational complexity can be resolved by high-speed processors and low complex decoders [106].

3.1.4 Remarks on CSI Requirement

The CSI requirements of the nodes in the cooperative D2D system are as follows.

- *CSI requirement of source node:* The source node requires the average CSI of the channel between itself to relay nodes. This CSI is useful for probabilistic relay selection. In practice, the required CSI can be acquired by channel estimation using training or pilot sequences [107].

- *CSI requirement of relay node:* The selected PA-DAF relay has to acquire accurate instantaneous CSI of the source to the relay link for successful decoding of its received signal. Furthermore, the selected PA-DAF relay node has also to acquire instantaneous CSI of both the relays to the destination link to set transmit power optimally. In practice, the node can employ a training protocol for the CSI acquisition. However, the selected relay need not know instantaneous CSI of the source to the unselected relay node.

- *CSI requirement of destination node:* Destination node also requires instantaneous CSI between selected PA-DAF relay to the destination link, to decode the received signal at the destination.

3.1.5 Remarks on PRSP Design and Analysis

A wide range of relay selection policies exists in the literature on cooperative systems. Most of these policies require excessive overhead information exchange between the nodes along with high processing capabilities requirement for the relay nodes.

Therefore, to support excessive overhead information exchange and enhanced processing capabilities, highly complex relay nodes are required with increased resource utilization. Such necessities make the system less friendly and less feasible in terms of practical implementation. Hence, keeping these issues in mind, we use PRSP, which reduces the excessive overhead exchange demand and in turn, reduces the relay node complexity.

Table 3.2: Relay selection criterion in PRSP when frequency-flat Rayleigh fading channels is assumed.

Relay Node Selected	Selection Criterion	Comments
R_1	$\mathcal{P}(\Gamma_{R_1} > \Gamma_{R_2}) \triangleq w_1$, $w_1 = \frac{\overline{\gamma}_{d_1r_1}}{\overline{\gamma}_{d_1r_1}+\overline{\gamma}_{d_1r_2}}$,	Relay R_1 is selected, if the probability for instantaneous SNR of $\Gamma_{d_1r_1}$ is greater than instantaneous SNR of $\Gamma_{d_1r_2}$.
R_2	$\mathcal{P}(\Gamma_{R_1} < \Gamma_{R_2}) \triangleq w_2$, $w_2 = \frac{\overline{\gamma}_{d_1r_2}}{\overline{\gamma}_{d_1r_1}+\overline{\gamma}_{d_1r_2}}$,	Relay R_2 is selected, if the probability for instantaneous SNR of $\Gamma_{d_1r_2}$ is greater than instantaneous SNR of $\Gamma_{d_1r_1}$.

To understand PRSP, we first define the instantaneous SNR of D_1-R_1 and D_1-R_2 links. The SNR of D_1-R_1 and D_1-R_2 links are given by

$$\Gamma_{R_1} = \frac{\tilde{P}_{d_1}\gamma_{d_1r_1}}{{\sigma_n}^2}, \quad \Gamma_{R_2} = \frac{\tilde{P}_{d_1}\gamma_{d_1r_2}}{{\sigma_n}^2}, \tag{3.1.1}$$

where $\gamma_{d_1r_1}$, and $\gamma_{d_1r_2}$, are instantaneous channel power gain of D_1-R_1 link, and D_1-R_2 link, respectively and σ_n^2 is the noise variance. Furthermore, $\overline{\gamma}_{d_1r_1}$, and $\overline{\gamma}_{d_1r_2}$, are the mean channel power gain of D_1-R_1 link, and D_1-R_2 link, respectively. Selection of the best relay based on PRSP is described in Table 3.2.

Remarks on the nature of relay selection policy: Note that the relay selection will not fall in the optimal relay selection scheme. The relay selection is not optimal because the PA-DAF relay is selected based on the partial CSI and is a PRSP. However, the selected PA-DAF relay optimally sets its relay gain to optimize the end performance of the cooperative D2D system. In summary, while the relay selection is a simple PRSP, the PA-DAF relaying that happens after relay selection is optimal.

3.2 Fading Averaged Performance Measures, Optimization, and Analysis

Several performance measures are proposed in the literature on the PHY layer performance of cooperative wireless systems. These performance measures include symbol error rate, spectral efficiency, energy efficiency, outage probability. Among these, we focus on i) FASER, ii) FASE, and iii) FAEE.

The rationale behind choosing the above mentioned PHY layer performance measures is because wireless fading channel is random and causes attenuation of transmitted signal strength as it propagates through the channel. Therefore, the instantaneous measures do not provide useful insights on the system performance for time-varying fading channels. On the other hand, FASER, FASE, and FAEE, which are evaluated after averaging over channel fading, provide valuable information on the link reliability, bandwidth utilization, and energy efficiency, respectively.

We consider each of the performance measures independently and develop optimization problem, solution and performance analysis. Specifically, we come up with an averaged power constrained optimization problem and derive its solution, which we call as optimal relaying policy. The selected PA-DAF relay sets the optimal relay gain, which is the unique positive solution of the equation defined by the policy. We denote the optimal solution, that is, the optimal RGF, as $\mathcal{G}_x^*(\gamma_1, \gamma_2), x \in \{\beta, \eta, \mathcal{E}\}$ for each performance measure. In the following section, we formally state the optimization problem and derive its optimal solution.

3.2.1 FASER Minimization Problem and Analysis for MPSK

The instantaneous SNRs of the signal received at the destination via $R_1 - D_2$ and $R_2 - D_2$ links are given by

$$\Gamma_1 = \frac{\mathcal{G}_x\left(\gamma_1, \gamma_2\right) \tilde{P}_r \gamma_1}{\sigma_n^2}, \quad \text{and} \quad \Gamma_2 = \frac{\mathcal{G}_x\left(\gamma_1, \gamma_2\right) \tilde{P}_r \gamma_2}{\sigma_n^2}, \tag{3.2.1}$$

where $\tilde{P}_r = \tilde{P}_{r_1} = \tilde{P}_{r_2}$ is power received at the destination after accounting for path loss. Furthermore, the relay transmit power $P_{r_1} = P_{r_2} = \mathcal{G}_x\left(\gamma_1, \gamma_2\right) P_r$.

The FASER measures the reliability of the link. It is the number of symbol errors per unit time. On average, the cooperative D2D wireless link turns out to be more reliable for lower FASER. Note that the FASER depends on the received SNR and gives the information regarding the symbol errors in the total received symbols due to noise and channel distortion created in the fading channel at a given point of time.

We now formally state the FASER minimization problem for MPSK constellation. Since the PA-DAF relays R_1, and R_2 are selected with probabilities w_1, and w_2, respectively, the exact FASER can be expressed as [108],

$$\text{FASER} = \mathbf{E}\left[\frac{w_1}{\pi}\int_0^{(\frac{M-1}{M})\pi} \exp\left(-\mathcal{M}\Gamma_1 \csc^2\theta\right)\, d\theta + \frac{w_2}{\pi}\int_0^{(\frac{M-1}{M})\pi} \exp\left(-\mathcal{M}\Gamma_2 \csc^2\theta\right)\, d\theta\right], \tag{3.2.2}$$

where $\mathcal{M} = \sin^2(\frac{\pi}{M})$, and M is the order of modulation. Note that FASER is a function of $\mathcal{G}_{\beta-\text{MPSK}}(\gamma_1, \gamma_2)$. For brevity and to conserve space, we do not show this dependence. Therefore, using the inequality $\sin^2\theta \leq 1$, the FASER in (3.2.2) can be upper bounded as

$$\text{FASER} \leq \frac{M-1}{M}\mathbf{E}\left[w_1 \exp\left(-\mathcal{M}\Gamma_1\right) + w_2 \exp\left(-\mathcal{M}\Gamma_2\right)\right]. \tag{3.2.3}$$

Mathematically, the constrained minimization problem for MPSK is given by

$$\min_{\mathcal{G}_{\beta-\text{MPSK}}(\gamma_1,\gamma_2)} \mathbf{E}\left[w_1 \exp\left(-\mathcal{M}\Gamma_1\right) + w_2 \exp\left(-\mathcal{M}\Gamma_2\right)\right], \tag{3.2.4}$$

$$\text{s.t. } \mathbf{E}\left[\mathcal{G}_{\beta-\text{MPSK}}\left(\gamma_1, \gamma_2\right)\tilde{P}_r\right] \leq P_{\text{th}}, \tag{3.2.5}$$

where $\mathcal{G}_{\beta-\text{MPSK}}(\gamma_1, \gamma_2)$ is the RGF for FASER MPSK constellation, and its optimum value is denoted by $\mathcal{G}^*_{\beta-\text{MPSK}}(\gamma_1, \gamma_2)$, and P_{th} is the threshold power. Since the optimization problem is convex, we use Lagrange multiplier technique to derive the optimum relaying policy that sets RGF $\mathcal{G}_{\beta-\text{MPSK}}(\gamma_1, \gamma_2)$ optimally.

The objective here is to minimize the upper bound of the FASER with respect to the RGF $\mathcal{G}_{\beta-\text{MPSK}}(\gamma_1, \gamma_2)$. Therefore, the optimal solution will also minimize the exact FASER. To conserve space, we denote the RGF $\mathcal{G}_{\beta-\text{MPSK}}(\gamma_1, \gamma_2)$ as simply, $\mathcal{G}_{\beta-\text{MPSK}}$.

Result 5 FASER optimal relaying policy for MPSK:

The optimal RGF that minimizes FASER is a unique positive solution of the following transcendental equation:

$$w_1\gamma_1\, c\, \exp\left(-\, c\gamma_1\mathcal{G}^*_{\beta-MPSK}\right) + w_2\gamma_2\, c\, \exp\left(-\, c\gamma_2\mathcal{G}^*_{\beta-MPSK}\right) = K\tilde{P}_r, \tag{3.2.6}$$

where $K > 0$ is the Lagrange multiplier, and is chosen such that the average power constraint in equation (3.2.5) *should satisfy the equality and $c \triangleq \frac{\mathcal{M}\tilde{P}_r}{\sigma_n^2}$.*

Since equation (3.2.6) is transcendental in nature, we numerically solve it to determine the value of $\mathcal{G}^*_{\beta-\text{MPSK}}$. The proof the FASER-optimal policy is relegated in Appendix B.1.

Power conservation rule: If $w_1\gamma_1 + w_2\gamma_2 < \frac{K\tilde{P}_r}{c}$, then $\mathcal{G}^*_{\beta-\text{MPSK}} = 0$, that is, the relay does not participate in relaying process. Qualitatively, this rule implies that if the link quality between the relays and the destination node is not good, the relay should stop transmitting the signal to the destination node in order to conserve power.

After rearranging, we can re-write the PA-DAF relay OFF-condition as follows.

$$\gamma_2 \;<\; \rho(\gamma_1) \;\triangleq \frac{K\tilde{P}_r - w_1\gamma_1\, c}{w_2\, c}. \tag{3.2.7}$$

After obtaining the value of $\mathcal{G}^*_{\beta-\text{MPSK}}$ and considering the power conservation condition, we can now determine the FASER expression for the system model considered using Craig's formula.

Result 6 Exact FASER and its upper bound for MPSK:

Exact FASER analytical expression for MPSK modulation is given by

$$\begin{aligned}
&\text{FASER}_{\text{MPSK}} = \\
&\frac{w_1}{\pi\overline{\gamma}_1\overline{\gamma}_2}\left[\frac{\pi\overline{\gamma}_1\overline{\gamma}_2(M-1)}{M}\mathbb{R} + \int_{\theta=0}^{\left(\frac{M-1}{M}\right)\pi}\int_{\gamma_1=0}^{\infty}\int_{\gamma_2=\rho(\gamma_1)}^{\infty} e^{-\mathcal{W}\gamma_1}e^{-\frac{\gamma_1}{\overline{\gamma}_1}}e^{-\frac{\gamma_2}{\overline{\gamma}_2}}d\gamma_2 d\gamma_1 d\theta\right] \\
&+ \frac{w_2}{\pi\overline{\gamma}_1\overline{\gamma}_2}\left[\frac{\pi\overline{\gamma}_1\overline{\gamma}_2(M-1)}{M}\mathbb{R} + \int_{\theta=0}^{\left(\frac{M-1}{M}\right)\pi}\int_{\gamma_1=0}^{\infty}\int_{\gamma_2=\rho(\gamma_1)}^{\infty} e^{-\mathcal{W}\gamma_2}e^{-\frac{\gamma_1}{\overline{\gamma}_1}}e^{-\frac{\gamma_2}{\overline{\gamma}_2}}d\gamma_2 d\gamma_1 d\theta\right],
\end{aligned} \tag{3.2.8}$$

where $\mathbb{R} = \left[1 + \frac{w_2\overline{\gamma}_2 e^{\frac{-K\sigma_n^2}{w_2\overline{\gamma}_2\mathcal{M}}}}{w_1\overline{\gamma}_1 - w_2\overline{\gamma}_2}\right]$, $\mathcal{W} = c\,\mathcal{G}^*_{\beta-MPSK}\csc^2\theta$, $\overline{\gamma}_1$ *is the average channel power gain of* $R_1 - D_2$ *link and* $\overline{\gamma}_2$ *is the average channel power gain of* $R_2 - D_2$ *link.*

Furthermore, the upper bound for the $FASER_{UB\text{-}MPSK}$ *is given by*

$$\begin{aligned}
&\text{FASER}_{\text{UB}-\text{MPSK}} = \\
&\frac{w_1}{\pi\overline{\gamma}_1\overline{\gamma}_2}\left[\frac{\pi\overline{\gamma}_1\overline{\gamma}_2(M-1)}{M}\mathbb{R} + \left(\frac{M-1}{M}\right)\pi\int_{\gamma_1=0}^{\infty}\int_{\gamma_2=\rho(\gamma_1)}^{\infty} e^{-\mathbb{W}\gamma_1}e^{-\frac{\gamma_1}{\overline{\gamma}_1}}e^{-\frac{\gamma_2}{\overline{\gamma}_2}}\, d\gamma_2\, d\gamma_1\right] \\
&+ \frac{w_2}{\pi\overline{\gamma}_1\overline{\gamma}_2}\left[\frac{\pi\overline{\gamma}_1\overline{\gamma}_2(M-1)}{M}\mathbb{R} + \left(\frac{M-1}{M}\right)\pi\int_{\gamma_1=0}^{\infty}\int_{\gamma_2=\rho(\gamma_1)}^{\infty} e^{-\mathbb{W}\gamma_2}e^{-\frac{\gamma_1}{\overline{\gamma}_1}}e^{-\frac{\gamma_2}{\overline{\gamma}_2}}d\gamma_2\, d\gamma_1\right].
\end{aligned} \tag{3.2.9}$$

where $\mathbb{W} = c\mathcal{G}^*_{\beta-MPSK}$.

The proof for the exact FASER and its upper bound is relegated in appendix B.2.

Remarks: Since the exact FASER and its upper bound is difficult to simplify

further, therefore both can be computed numerically. We evaluate the analytical results numerically in section 3.3.

3.2.2 Diversity order analysis in a scaling regime:

Diversity order analysis provides in-depth and useful insights regarding the robustness against the large scale and small scale fading of the proposed cooperative D2D model. Mathematically

$$\text{FASER} \propto \frac{1}{\overline{\Gamma}^{L}} \ , \tag{3.2.10}$$

where L is the diversity order, and $\overline{\Gamma}$ is the average received SNR at the destination in the high SNR regime [109].

We now prove the diversity order for PA-DAF relay-assisted cooperative D2D communication network with PRSP relay selection in high SNR regime. For it, we assume that, $\tilde{P}_r \to \infty$, average SNRs of $R_1 - D_2$ link and $R_2 - D_2$ link, that is, $\overline{\Gamma}_1$ and $\overline{\Gamma}_2$, respectively, are very high and equal, that is, $\overline{\Gamma}_1 = \overline{\Gamma}_2 = \overline{\Gamma}$ and all other parameters are fixed.

We see that the diversity order of FASER upper bound is one since the diversity order for the sub-optimal policy is also one [108]. We now show that the lower bound also achieves diversity order one in the scaling regime.

From equation (3.2.1) and (3.2.2), the $\text{FASER}_{\text{MPSK}}$ can be expressed as

$$\begin{aligned}\text{FASER}_{\text{MPSK}} = \mathbf{E}\bigg[\int_0^{(\frac{M-1}{M})\pi} \frac{w_1}{\pi} \exp\Big(-\frac{\mathcal{M}\mathcal{G}^*_{\beta}(\gamma_1,\gamma_2)\ \tilde{P}_r\gamma_1}{\sigma_n^2 \csc^2\theta}\Big)\mathrm{d}\theta\bigg] \\ + \mathbf{E}\bigg[\int_0^{(\frac{M-1}{M})\pi} \frac{w_2}{\pi} \exp\Big(-\frac{\mathcal{M}\mathcal{G}^*_{\beta}(\gamma_1,\gamma_2)\ \tilde{P}_r\gamma_2}{\sigma_n^2 \csc^2\theta}\Big)\mathrm{d}\theta\bigg].\end{aligned} \tag{3.2.11}$$

To obtain lower bound, we replace $\sin^2\theta$ with its lower bound value, that is $\frac{1}{2}$, for $\frac{\pi}{4} \le \theta \le \frac{3\pi}{4}$, and 0 for $0 \le \theta \le \frac{\pi}{4}$ and $\frac{3\pi}{4} \le \theta \le \pi$. Therefore, the exact $\text{FASER}_{\text{MPSK}}$ can be lower bounded as

$$\begin{aligned}\text{FASER}_{\text{MPSK}} \ge \frac{w_1}{2}\mathbf{E}\bigg[\ \exp\Big(-\frac{2\mathcal{M}\mathcal{G}^*_{\beta}(\gamma_1,\gamma_2)\ \tilde{P}_r\gamma_1}{\sigma_n^2}\Big)\bigg] \\ + \frac{w_2}{2}\mathbf{E}\bigg[\ \exp\Big(-\frac{2\mathcal{M}\mathcal{G}^*_{\beta}(\gamma_1,\gamma_2)\ \tilde{P}_r\gamma_2}{\sigma_n^2}\Big)\bigg] \triangleq \text{FASER}_{\text{LB-MPSK}}\end{aligned} \tag{3.2.12}$$

Furthermore, expanding the expectation term, the above lower bound expression can

be expressed as

$$\begin{aligned}\text{FASER}_{\text{LB-MPSK}} = \frac{w_1}{2\overline{\gamma}_1\overline{\gamma}_2}\int_0^\infty\int_0^\infty e^{\left(-\frac{2\mathcal{M}\mathcal{G}^*_\beta(\gamma_1,\gamma_2)\ \tilde{P}_r\gamma_1}{\sigma_n^2}\right)}\ e^{-\frac{\gamma_1}{\overline{\gamma}_1}}\ e^{-\frac{\gamma_2}{\overline{\gamma}_2}}\mathrm{d}\gamma_1\ \mathrm{d}\gamma_2 \\ + \frac{w_2}{2\overline{\gamma}_1\overline{\gamma}_2}\int_0^\infty\int_0^\infty e^{\left(-\frac{2\mathcal{M}\mathcal{G}^*_\beta(\gamma_1,\gamma_2)\ \tilde{P}_r\gamma_2}{\sigma_n^2}\right)}\ e^{-\frac{\gamma_1}{\overline{\gamma}_1}}\ e^{-\frac{\gamma_2}{\overline{\gamma}_2}}\mathrm{d}\gamma_1\ \mathrm{d}\gamma_2.\end{aligned} \tag{3.2.13}$$

In the scaling regime, as $\tilde{P}_r \to \infty$, $\mathcal{G}^*_\beta(\gamma_1,\gamma_2) \to \mathcal{V}$, a positive constant. Further simplification yields

$$\text{FASER}_{\text{LB-MPSK}} = \frac{w_1}{2}\left[\frac{\sigma_n^2}{2\mathcal{M}\mathcal{V}\tilde{P}_r\overline{\gamma}_1+\sigma_n^2}\right] + \frac{w_2}{2}\left[\frac{\sigma_n^2}{2\mathcal{M}\mathcal{V}\tilde{P}_r\overline{\gamma}_2+\sigma_n^2}\right]. \tag{3.2.14}$$

Let $\overline{\Gamma}_1 = \overline{\Gamma}_2 = \overline{\Gamma}$ and $\overline{\gamma}_1 = \overline{\gamma}_2 = \overline{\gamma}$. Further simplification yields

$$\begin{aligned}\text{FASER}_{\text{LB-MPSK}} &= \frac{w_1}{2}\left[\frac{\sigma_n^2}{2\mathcal{M}\mathcal{V}\tilde{P}_r\overline{\gamma}}\right] + \frac{w_2}{2}\left[\frac{\sigma_n^2}{2\mathcal{M}\mathcal{V}\tilde{P}_r\overline{\gamma}}\right], \\ &= \frac{w_1+w_2}{4\mathcal{M}}\left[\frac{1}{\overline{\Gamma}^1}\right].\end{aligned} \tag{3.2.15}$$

From the above expression, we see that the exponent of average SNR $\overline{\Gamma}$ is one. Thus, the diversity order for the lower bound is one. Since the diversity order of both upper bound and lower bound is one, the proposed model achieves diversity order one in the scaling regime.

3.2.3 FASER Analysis of MQAM

As discussed, to measure the link reliability, we analyze FASER. The information regarding the symbol errors in the total received symbols due to noise and channel distortion created in the fading channel at a given point of time is analyzed by FASER. The wireless link turns out to be more reliable if the value of FASER is low.

In this section, we present the FASER minimization problem for MQAM, solution for determining $\mathcal{G}^*_{\beta-\text{MQAM}}(\gamma_1,\gamma_2)$, and an analytical expression for FASER. For MQAM constellation, the FASER minimization problem is mathematically represented as

$$\min_{\mathcal{G}(\gamma_1,\gamma_2)} \mathbf{E}\ \left(w_1\exp\left(-m'\Gamma_1\right) + w_2\exp\left(-m'\Gamma_2\right)\right), \tag{3.2.16}$$

$$\text{s.t. } \mathbf{E}\left[\mathcal{G}_{\beta-\text{MQAM}}(\gamma_1,\gamma_2)\ \tilde{P}_r\right] \le P_{\text{th}}, \tag{3.2.17}$$

where $\mathcal{G}_{\beta-\text{MQAM}}(\gamma_1, \gamma_2)$ is the RGF and $m^{'} = \frac{3}{2(M-1)}$. As in the case of MPSK, the optimization problem of MQAM constellation is also convex, therefore we use convex optimization technique to obtain the optimum value of $\mathcal{G}_{\beta-\text{MQAM}}(\gamma_1, \gamma_2)$ that is, $\mathcal{G}^*_{\beta-\text{MQAM}}(\gamma_1, \gamma_2)$. To conserve space we will be representing $\mathcal{G}_{\beta-\text{MQAM}}(\gamma_1, \gamma_2)$ by $\mathcal{G}_{\beta-\text{MQAM}}$.

Result 7 FASER optimal relaying policy for MQAM: *The optimal RGF that minimizes FASER for MQAM constellation is a unique positive solution of the following transcendental equation:*

$$w_1\gamma_1\ c^{'} \exp\left(-\ c^{'}\gamma_1\mathcal{G}^*_{\beta-MQAM}\ \right) + w_2\gamma_2\ c^{'} \exp\left(-\ c^{'}\gamma_2\mathcal{G}^*_{\beta-MQAM}\ \right) = K^{'}\tilde{P}_r, \qquad (3.2.18)$$

where $K^{'}$ is positive constant which should satisfy power equality constraint of equation (3.2.17) *and $c^{'} = \frac{m^{'}\tilde{P}_r}{\sigma_n^2}$. Proof of this equation is relegated in appendix B.4.*

Remarks: We note that the FASER optimal policy for MPSK, and MQAM have similar structure in the sense that both the policies contain transcendental equations to be solved numerically. However, the power conservation rules and optimal solutions are different. Since both MPSK and MQAM constellations are widely used in various wireless systems, both the optimal policies are important and useful for the next generation cooperative D2D systems.

Power conservation rule: To conserve the power in scenarios where the link quality is not good for the transmission, the power saving rule states that $\mathcal{G}^*_{\beta-\text{MQAM}} = 0$ for $w_1\gamma_1\ c^{'} + w_2\gamma_2\ c^{'}\ <\ K^{'}\tilde{P}_r$. After re-arranging, we get

$$\gamma_2\ <\ \rho^{'}(\gamma_1)\ \triangleq \frac{K^{'}\tilde{P}_r - w_1\gamma_1\ c^{'}}{w_2\ c^{'}}. \qquad (3.2.19)$$

Once the optimum value of $\mathcal{G}_{\beta-\text{MQAM}}$ is obtained numerically, we then compute the exact FASER. We now state the analytical expressions for exact FASER and its upper bound.

Result 8 Exact FASER and its upper bound for MQAM: *The exact FASER analytical expression for MQAM constellation is given below.*

$$\begin{aligned}\text{FASER}_{\text{MQAM}} = \frac{4m^2}{\pi\overline{\gamma}_1\overline{\gamma}_2}\Bigg[\frac{w_1}{m}\Bigg[\mathcal{F}+\int_{\theta=0}^{\frac{\pi}{2}}\int_{\gamma_1=0}^{\infty}\int_{\gamma_2=\rho'(\gamma_1)}^{\infty} e^{-\mathcal{Y}\gamma_1}e^{-\frac{\gamma_1}{\overline{\gamma}_1}}e^{-\frac{\gamma_2}{\overline{\gamma}_2}}d\gamma_2\ d\gamma_1 d\theta\Bigg] \\ - w_1\Bigg[\frac{\mathcal{F}}{2}+\int_{\theta=0}^{\frac{\pi}{4}}\int_{\gamma_1=0}^{\infty}\int_{\gamma_2=\rho'(\gamma_1)}^{\infty} e^{-\mathcal{Y}\gamma_1}e^{-\frac{\gamma_1}{\overline{\gamma}_1}}e^{-\frac{\gamma_2}{\overline{\gamma}_2}}d\gamma_2 d\gamma_1 d\theta\Bigg] \\ + \frac{w_2}{m}\Bigg[\mathcal{F}+\int_{\theta=0}^{\frac{\pi}{2}}\int_{\gamma_1=0}^{\infty}\int_{\gamma_2=\rho'(\gamma_1)}^{\infty} e^{-\mathcal{Y}\gamma_2}e^{-\frac{\gamma_1}{\overline{\gamma}_1}}e^{-\frac{\gamma_2}{\overline{\gamma}_2}}d\gamma_2 d\gamma_1 d\theta\Bigg] \\ - w_2\Bigg[\frac{\mathcal{F}}{2}+\int_{\theta=0}^{\frac{\pi}{4}}\int_{\gamma_1=0}^{\infty}\int_{\gamma_2=\rho'(\gamma_1)}^{\infty} e^{-\mathcal{Y}\gamma_2}e^{-\frac{\gamma_1}{\overline{\gamma}_1}}e^{-\frac{\gamma_2}{\overline{\gamma}_2}}d\gamma_2 d\gamma_1 d\theta\Bigg]\Bigg], \quad (3.2.20)\end{aligned}$$

where $m = 1 - \frac{1}{\sqrt{M}}$, $\mathcal{Y} = c'\ \mathcal{G}^*_{\beta-MQAM}\csc^2\theta$, *and* $\mathcal{F} \triangleq \pi\overline{\gamma}_1\overline{\gamma}_2\frac{(M-1)}{M}\left[1+\frac{w_2\overline{\gamma}_2 e^{\frac{-\kappa\sigma_n^2}{w_2\overline{\gamma}_2 M}}}{w_1\overline{\gamma}_1 - w_2\overline{\gamma}_2}\right]$.

Further, the FASER upper bound expression can be written as

$$\begin{aligned}\text{FASER}_{\text{UB-MQAM}} = \frac{4m^2}{\pi\overline{\gamma}_1\overline{\gamma}_2}\Bigg[\frac{w_1}{m}\Bigg[\mathcal{F}+\frac{\pi}{2}\int_{\gamma_1=0}^{\infty}\int_{\gamma_2=\rho'(\gamma_1)}^{\infty} e^{-\mathbb{Y}\gamma_1}e^{-\frac{\gamma_1}{\overline{\gamma}_1}}e^{-\frac{\gamma_2}{\overline{\gamma}_2}}d\gamma_2 d\gamma_1\Bigg] \\ - w_1\Bigg[\frac{\mathcal{F}}{2}+\frac{\pi}{4}\int_{\gamma_1=0}^{\infty}\int_{\gamma_2=\rho'(\gamma_1)}^{\infty} e^{-\mathbb{Y}\gamma_1}e^{-\frac{\gamma_1}{\overline{\gamma}_1}}e^{-\frac{\gamma_2}{\overline{\gamma}_2}}d\gamma_2 d\gamma_1\Bigg] \\ + \frac{w_2}{m}\Bigg[\mathcal{F}+\frac{\pi}{2}\int_{\gamma_1=0}^{\infty}\int_{\gamma_2=\rho'(\gamma_1)}^{\infty} e^{-\mathbb{Y}\gamma_2}e^{-\frac{\gamma_1}{\overline{\gamma}_1}}\ e^{-\frac{\gamma_2}{\overline{\gamma}_2}}d\gamma_2 d\gamma_1\Bigg] \\ - w_2\Bigg[\frac{\mathcal{F}}{2}+\frac{\pi}{4}\int_{\gamma_1=0}^{\infty}\int_{\gamma_2=\rho'(\gamma_1)}^{\infty} e^{-\mathbb{Y}\gamma_2}e^{-\frac{\gamma_1}{\overline{\gamma}_1}}e^{-\frac{\gamma_2}{\overline{\gamma}_2}}d\gamma_2 d\gamma_1\Bigg]\Bigg]. \quad (3.2.21)\end{aligned}$$

where $\mathbb{Y} = c'\mathcal{G}^*_{\beta-MQAM}$.

Proofs of the exact FASER and its upper bound are relegated in appendix B.5.

3.2.4 Fading Averaged Spectral Efficiency Analysis

Average spectral efficiency provides information regarding the ability of the cooperative D2D communication system to deliver information rate (in bits per second) for given bandwidth (in Hz). This section deals with deriving the optimal RGF that is, $\mathcal{G}^*_\eta(\gamma_1,\gamma_2)$ for the FASE performance measure. To get the optimized value of $\mathcal{G}_\eta(\gamma_1,\gamma_2)$, we first define the maximization problem for FASE and then solve it. Once the $\mathcal{G}^*_\eta(\gamma_1,\gamma_2)$ is obtained, we use this value to determine the FASE for the proposed

policy. The optimization problem can be represented as

$$\max_{\mathcal{G}_\eta(\gamma_1,\gamma_2)} \mathbf{E}\left[w_1 \log_2\left(1+\Gamma_1\right) + w_2 \log_2\left(1+\Gamma_2\right)\right], \tag{3.2.22}$$

$$\text{s.t. } \mathbf{E}\left[\mathcal{G}_\eta\left(\gamma_1,\gamma_2\right)\tilde{P}_r\right] \leq P_{\text{th}}. \tag{3.2.23}$$

As can be observed, the FASE maximization problem is concave. We reformulate it into a convex optimization problem by just negating the objective function in (3.2.22) and solving it to obtain $\mathcal{G}_\eta^*\left(\gamma_1,\gamma_2\right)$. From now on, we represent $\mathcal{G}_\eta^*\left(\gamma_1,\gamma_2\right)$ by $\mathcal{G}_\eta^*$ to conserve space.

Result 9 FASE optimal relaying policy:

The optimal RGF that maximizes FASE is a unique positive solution of the following quadratic equation:

$$\mathcal{A}{\mathcal{G}_\eta}^2 + \mathcal{B}\mathcal{G}_\eta + \mathcal{C} = 0, \tag{3.2.24}$$

where

$$\begin{aligned}
\mathcal{A} &\triangleq {\tilde{P}_r}^2 \gamma_1\gamma_2\mathcal{T}\ln(2),\\
\mathcal{B} &\triangleq \tilde{P}_r\gamma_1\sigma_n^2\mathcal{T}\ln(2) + \tilde{P}_r\gamma_2\sigma_n^2\mathcal{T}\ln(2) - \tilde{P}_r\gamma_1\gamma_2\\
\mathcal{C} &\triangleq \sigma_n^4\mathcal{T}\ln(2) - w_1\gamma_1\sigma_n^2 - w_2\gamma_2\sigma_n^2.
\end{aligned}$$

Note $\mathcal{T} > 0$, and its value should be kept such that it must satisfy the average power constraint with equality (3.2.23)*. We now have a quadratic equation. The unique positive root is the optimum solution of $\mathcal{G}_\eta$. Proof of the above result is relegated in appendix B.6.*

Remarks: We note that the FASE optimal policy, unlike FASER optimal policies, has different structure. Specifically, the FASE optimal solution is in close form and hence less complex. The FASE optimal policy can be applied to bandwidth limited cooperative D2D wireless systems to improve spectral efficiency.

Power conservation rule: For conserving power, we state the following rule. We have $\mathcal{G}_\eta^* = 0$ for $w_1\gamma_1 + w_2\gamma_2 < \mathcal{T}\sigma_n^2\ln(2)$. After re-arranging, we get

$$\mathcal{L}(\gamma_1) \triangleq \gamma_2 < \frac{\sigma_n^2\mathcal{T}\ln(2) - w_1\gamma_1}{w_2}. \tag{3.2.25}$$

Result 10 Exact FASE expression and its upper bound:

The exact analytical expression for FASE is as follows:

$$\overline{\mathcal{S}}_{\eta} = \frac{1}{\bar{\gamma}_1\bar{\gamma}_2\ln(2)}\Bigg[w_1\int_{\gamma_1=0}^{\infty}\int_{\gamma_2=\mathcal{L}(\gamma_1)}^{\infty}\ln\left(1+\frac{\mathcal{G}_{\eta}^{*}\tilde{P}_r\gamma_1}{\sigma_n^2}\right)e^{-\frac{\gamma_1}{\bar{\gamma}_1}}e^{-\frac{\gamma_2}{\bar{\gamma}_2}}\,d\gamma_2\,d\gamma_1 + w_2\int_{\gamma_1=0}^{\infty}\int_{\gamma_2=\mathcal{L}(\gamma_1)}^{\infty}\ln\left(1+\frac{\mathcal{G}_{\eta}^{*}\tilde{P}_r\gamma_2}{\sigma_n^2}\right)e^{-\frac{\gamma_1}{\bar{\gamma}_1}}e^{-\frac{\gamma_2}{\bar{\gamma}_2}}\,d\gamma_2\,d\gamma_1\Bigg]. \quad (3.2.26)$$

Furthermore, the upper bound for FASE is given by

$$\overline{\mathcal{S}}_{\eta-\mathrm{UB}} = \frac{1}{\ln(2)}\Bigg[w_1\ln\left(1+\frac{1}{\bar{\gamma}_1\bar{\gamma}_2}\int_{\gamma_1=0}^{\infty}\int_{\gamma_2=\mathcal{L}(\gamma_1)}^{\infty}\frac{\mathcal{G}_{\eta}^{*}\tilde{P}_r\gamma_1}{\sigma_n^2}\,e^{-\frac{\gamma_1}{\bar{\gamma}_1}}\,e^{-\frac{\gamma_2}{\bar{\gamma}_2}}d\gamma_2\,d\gamma_1\right) + w_2\ln\left(1+\frac{1}{\bar{\gamma}_1\bar{\gamma}_2}\int_{\gamma_1=0}^{\infty}\int_{\gamma_2=\mathcal{L}(\gamma_1)}^{\infty}\frac{\mathcal{G}_{\eta}^{*}\tilde{P}_r\gamma_2}{\sigma_n^2}\,e^{-\frac{\gamma_1}{\bar{\gamma}_1}}e^{-\frac{\gamma_2}{\bar{\gamma}_2}}d\gamma_2\,d\gamma_1\right)\Bigg]. \quad (3.2.27)$$

Proof of the above expression is relegated in appendix B.7.

Remarks: A double integral expression is derived for the exact FASE as well as its upper bound. Further simplification can be done numerically. Note that the FASE is not dependent on modulation order M. Therefore the above derived expression is fit for different modulation schemes.

3.2.5 Fading Averaged Energy Efficiency Analysis

In this section, we analyze another important PHY layer performance measure that is, FAEE, which is closely associated with FASE. Instantaneous Energy Efficiency of a given network is defined as the ratio of instantaneous spectral efficiency to the total instantaneous power consumption. If we consider P_T as the total instantaneous power consumption in the network, then the FAEE that is, $\overline{\mathcal{E}}$ can be mathematically written as

$$\overline{\mathcal{E}} = \mathbf{E}\left(\frac{\mathcal{S}_{\eta}}{P_T}\right). \quad (3.2.28)$$

In this analysis, P_T is the sum of three instantaneous powers that is, i). instantaneous source transmit power, ii). instantaneous transmit power of relay, and iii). instantaneous circuitry power. Now, to maximize the FAEE for the proposed model, we first define the maximization problem, which is given by,

$$\max_{\mathcal{G}_{\mathcal{E}}(\gamma_1,\gamma_2)} \mathbf{E}\left(\frac{\mathcal{S}_{\eta}}{P_T}\right), \quad (3.2.29)$$

$$\text{s.t. } \mathbf{E}\Big[\mathcal{G}_{\mathcal{E}}(\gamma_1,\gamma_2)\;\tilde{P}_r\Big] \leq P_{\mathrm{th}}, \quad (3.2.30)$$

where $\mathcal{G}_{\mathcal{E}}(\gamma_1, \gamma_2)$ is the RGF to maximize FAEE and P_{th} is the threshold transmit power of the relay nodes (relay cannot transmit above P_{th}). Substituting the expression of instantaneous spectral efficiency and instantaneous total power consumed in equation (3.2.29), the above expression becomes,

$$\max_{\mathcal{G}_{\mathcal{E}}(\gamma_1,\gamma_2)} \mathbf{E}\left(\frac{w_1 \log_2(1+\Gamma_1) + w_2 \log_2(1+\Gamma_2)}{P_{d_1} + \mathcal{G}_{\mathcal{E}}(\gamma_1,\gamma_2)\ \tilde{P}_r + P_c}\right), \tag{3.2.31}$$

$$\text{s.t. } \mathbf{E}\left[\mathcal{G}_{\mathcal{E}}(\gamma_1,\gamma_2)\ \tilde{P}_r\right] \leq P_{\text{th}}, \tag{3.2.32}$$

where P_{d_1} is the source transmit power, P_r is the relay transmit power and P_c is the power consumed by the circuitry. As can be observed, the FAEE optimization problem is concave. We are converting it into a convex optimization problem and solving it to obtain $\mathcal{G}_{\mathcal{E}}^*(\gamma_1, \gamma_2)$. Note that from now on we are representing $\mathcal{G}_{\mathcal{E}}^*(\gamma_1, \gamma_2)$ as $\mathcal{G}_{\mathcal{E}}^*$ to conserve space.

We reformulate the above power-constrained concave optimization problem (3.2.31) into a convex optimization problem by just negating the objective function. We state the optimal policy that sets the optimal relay gain $\mathcal{G}_{\mathcal{E}}{}^*$ below.

Result 11 FAEE optimal relaying policy:

The optimal RGF that maximizes FAEE is a unique positive solution of the following transcendental equation:

$$w_1\left[\frac{\gamma_1}{\sigma_n^2 + \mathcal{G}_{\mathcal{E}}\tilde{P}_r\gamma_1} - \frac{\ln\left(1+\frac{\mathcal{G}_{\mathcal{E}}\tilde{P}_r\gamma_1}{\sigma_n^2}\right)}{P_{d_1} + \mathcal{G}_{\mathcal{E}}\tilde{P}_r + P_c}\right] + w_2\left[\frac{\gamma_2}{\sigma_n^2 + \mathcal{G}_{\mathcal{E}}\tilde{P}_r\gamma_2} - \frac{\ln\left(1+\frac{\mathcal{G}_{\mathcal{E}}\tilde{P}_r\gamma_2}{\sigma_n^2}\right)}{P_{d_1} + \mathcal{G}_{\mathcal{E}}\tilde{P}_r + P_c}\right]$$
$$= \mathcal{D}(P_{d_1} + \mathcal{G}_{\mathcal{E}}\tilde{P}_r + P_c)\ln(2). \tag{3.2.33}$$

Note that the above equation is transcendental equation and can be solved further numerically. From the above equation (3.2.33)*, the optimum value of $\mathcal{G}_{\mathcal{E}}$ which is denoted by $\mathcal{G}_{\mathcal{E}}^*$ can be obtained. Moreover, the value of Lagrange multiplier that is, $\mathcal{D}$ is obtained such that, it should be positive and should satisfy the power constraint of equation* (3.2.32)*. Proof of the above equation is relegated in appendix B.8.*

Remarks: We note that the FAEE optimal policy is different from FASE optimal policy. The FAEE optimal policy provides optimal relay gain that maximizes average energy efficiency. However, we need to numerically determine the optimal solution by solving the transcendental equation in (3.2.33). The FAEE optimal policy can be applied to power limited cooperative D2D green wireless systems to improve energy efficiency.

Power conservation rule: For conserving power, we assume a condition for power

conservation which is given by $\mathcal{G}_{\mathcal{E}}^{*}=0$ if $w_1\gamma_1+w_2\gamma_2<\mathcal{D}\ \sigma_n^2\ (P_{d_1}+P_c)\ln(2)$. This condition states that, if the channel conditions are not good, in this case, the relay should conserve its power by restraining itself from forwarding the received signal to the destination. Rearranging the power conservation expression, we get

$$\mathbb{H}(\gamma_1)\triangleq\gamma_2<\frac{\mathcal{D}\ \sigma_n^2\ (P_{d_1}+P_c)\ln(2)-w_1\ \gamma_1}{w_2}. \tag{3.2.34}$$

Therefore, based on the optimum RGF $\mathcal{G}_{\mathcal{E}}^{*}$ and power conservation condition, the FAEE for the proposed model can be derived.

Result 12 Exact FAEE and its upper bound:

The exact analytical expression for FAEE for the proposed model is given by

$$\begin{aligned}\overline{\mathcal{E}}=\frac{1}{\overline{\gamma}_1\overline{\gamma}_2\ln(2)}\Big[&w_1\int_{\gamma_1=0}^{\infty}\int_{\gamma_2=\mathbb{H}(\gamma_1)}^{\infty}\frac{ln\Big(1+\frac{\mathcal{G}_{\mathcal{E}}^{*}\ \tilde{P}_r\ \gamma_1}{\sigma_n^2}\Big)}{P_{d_1}+\mathcal{G}_{\mathcal{E}}^{*}\tilde{P}_r+P_c}\ e^{-\frac{\gamma_1}{\overline{\gamma}_1}}\ e^{-\frac{\gamma_2}{\overline{\gamma}_2}}d\gamma_2\ d\gamma_1\\&+w_2\int_{\gamma_1=0}^{\infty}\int_{\gamma_2=\mathbb{H}(\gamma_1)}^{\infty}\frac{ln\Big(1+\frac{\mathcal{G}_{\mathcal{E}}^{*}\ \tilde{P}_r\ \gamma_2}{\sigma_n^2}\Big)}{P_{d_1}+\mathcal{G}_{\mathcal{E}}^{*}\tilde{P}_r+P_c}\ e^{-\frac{\gamma_1}{\overline{\gamma}_1}}\ e^{-\frac{\gamma_2}{\overline{\gamma}_2}}d\gamma_2\ d\gamma_1\Big].\end{aligned} \tag{3.2.35}$$

Using the inequality $\ln(1+x)<x$ *for* $x>0$. *The upper bound of the above expression* (3.2.35) *can be written by*

$$\begin{aligned}\overline{\mathcal{E}}_{\mathrm{UB}}=\frac{1}{\overline{\gamma}_1\overline{\gamma}_2 ln(2)}\Big[&w_1\int_{\gamma_1=0}^{\infty}\int_{\gamma_2=\mathbb{H}(\gamma_1)}^{\infty}\frac{\Big(\frac{\mathcal{G}_{\mathcal{E}}^{*}\ \tilde{P}_r\ \gamma_1}{\sigma_n^2}\Big)}{P_{d_1}+\mathcal{G}_{\mathcal{E}}^{*}\tilde{P}_r+P_c}\ e^{-\frac{\gamma_1}{\overline{\gamma}_1}}\ e^{-\frac{\gamma_2}{\overline{\gamma}_2}}d\gamma_2\ d\gamma_1\\&+w_2\int_{\gamma_1=0}^{\infty}\int_{\gamma_2=\mathbb{H}(\gamma_1)}^{\infty}\frac{\Big(\frac{\mathcal{G}_{\mathcal{E}}^{*}\ \tilde{P}_r\ \gamma_2}{\sigma_n^2}\Big)}{P_{d_1}+\mathcal{G}_{\mathcal{E}}^{*}\tilde{P}_r+P_c}\ e^{-\frac{\gamma_1}{\overline{\gamma}_1}}\ e^{-\frac{\gamma_2}{\overline{\gamma}_2}}d\gamma_2\ d\gamma_1\Big].\end{aligned} \tag{3.2.36}$$

The proof of both the exact as well as the upper bound expression for FAEE is relegated in appendix B.9.

Remarks on the non closed-form expressions: Note that the exact analytical expressions for FASER, FASE, and FAEE cannot be simplified further in closed forms. This is because of the presence of optimal RGF $\mathcal{G}^{*}(\gamma_1,\gamma_2)$. However, the exact performance measures can be numerically evaluated using scientific packages such as Mathematica, MATLAB. Specifically, we use *fsolve* in MATLAB to determine the optimal gain value. In it, the computation efficiency depends on the numerical algorithm that *fsolve* uses, which is Trust-Region-Dogleg algorithm [110].

3.2.6 Computational Time, Complexity and Efficiency

In this chapter, we focus on optimizing the cooperative D2D system performance with respect to various popular PHY layer performance measures such as FASER, FASE, and FAEE. Furthermore, investigation of computational time, complexity, and efficiency are beyond the scope of our work. We present some useful remarks on computational time, complexity, and efficiency for various optimal policies.

The PA-DAF relay-assisted cooperative D2D system with PRSP involves three crucial computational tasks. These tasks are CSI acquisition, relay selection, and the computation of optimal gain. The computational complexity of the CSI acquisition depends on the channel estimation algorithm. For the relay selection, computation complexity of $\mathcal{O}(n\log_2(n))$ [111](where n is the number of relays in the system model), is possible for an optimal algorithm. Note that the relay selection problem is similar to finding the index of the maximum (or minimum) value (of the selection measure considered). Furthermore, the treatment of time complexity for computing the optimal relay gain is given below.

Computational time for PA-DAF relaying policy: Note that the computational time is more for FASER and FAEE policies than that of FASE policy. This increased complexity in time is because the former policies involve solving the transcendental equations. However, the computational time is less for FASE policy in which the optimal gain is a unique positive root of a quadratic equation. Therefore the computation time efficiency is upper bounded by $\mathcal{O}(n^2)$ [112] per channel realization for FASE policy. The reason for computation time efficiency being lesser than $\mathcal{O}(n^2)$ is due to the power conservation condition, which is given by $\mathcal{G}_{\eta}^{*}(\gamma_1,\gamma_2) = 0$ for $w_1\gamma_1 + w_2\gamma_2 < \mathcal{T}\sigma_n^2\ln(2)$. On the other hand, the computation efficiency of solving the transcendental equation per channel realization for FASER and FAEE depends on the numerical algorithm. For example, in MATLAB, we use fsolve that uses Trust-Region-Dogleg algorithm due to its computational efficiency [110].

The comparison table for the complexity of the proposed relaying policy and the fixed amplification DAF relaying policy is shown in Table 3.3. Note that the other simpler benchmark policies for the systems with only DF relays still has low time-complexity. However, the performance is more inferior. The above comparison Table 3.3 specifies the trade-off between complexity and performance in the relative sense. Thus, we see that the superior performance of the proposed policy comes with the expense of increased computational complexity. However, the benefits such as power savings scale up in a large-scale cooperative or cooperative and spectrum sharing communication networks.

Table 3.3: Complexity comparison of the proposed policy with respect to benchmark policy.

Model	Time Complexity	Hardware Complexity	Performance
PA-DAF Policy	High.	Medium.	Superior.
Fixed Amplification DAF Policy	Low.	Low.	Inferior.

Remarks on reducing computational complexity and improving efficiency: Computational complexity can be reduced, and computational efficiency can be improved by deriving simplified policies. For instance, consider the optimal solution for FASER optimization problem. Using the inequality $\exp(-x) \leq \frac{1}{1+x^2}$ for $x > 0$, a closed-form upper bound expression can be derived for $\mathcal{G}^*_\beta(\gamma_1, \gamma_2)$. The upper bound on optimal gain function reduce the computational complexity and enhance computational efficiency. The upper bound of optimal gain function with adjusted Lagrange parameter could serve as a simplified relaying policy, which is an approximate solution. Therefore, we have a trade-off between accuracy and computational complexity. Furthermore, the upper bound expressions that contain fewer integrals can be simplified to closed-form approximations using Gauss-Laguerre (G-L) quadrature [113].

3.3 Simulation Results and Discussion

In this section, we validate the derived analytical expressions and numerically evaluate the performance of the various optimal relaying policies in section 3.2. We validate analytical results using Monte-Carlo simulations (MCS). To quantify the performance gain quantitatively, we compare our proposed policy with various relaying policies; namely, conventional DAF relaying and fixed gain DAF relaying. Note that for the analysis, we have used PRSP as a relay selection policy for all the relaying scenarios. By extensive numerical results with benchmarking, we show that PA-DAF relaying policy outperforms other benchmark policies. Before presenting the performance plots, we describe simulation methodology of the proposed cooperative D2D system model.

3.3.1 Simulation Methodology

Below, we present a simulation methodology for the proposed model that involves several steps. These steps include simulation parameters declaration, source transmission model, relay selection and PA-DAF relaying model, and finally decoding and computation at the destination.

Initial parameter declaration: A list of simulation parameters is shown in Table 3.4. However, simulation parameters specific to a figure are included inside the caption.

Table 3.4: Simulation parameters for PA-DAF relay-assisted cooperative D2D communication system.

Simulation Parameter	Symbol	Value
Number of channel realizations	N	10^5
Constellation size	M	MPSK (M = 2) and M-QAM (M = 4 and 16)
Mean channel power gain	$\overline{\gamma}_i$ $(i \in 1, 2)$	1
Noise variance	σ_n^2	1
Threshold power	P_{th}	15 dB
Power consumed by the circuitry	P_c	15 dBm
Number of relays	R_i $(i \in 1, 2)$	2
Symbol energy	$\lvert\alpha\rvert^2$ (MPSK) $\mathbf{E}\lvert\alpha\rvert^2$ (MQAM)	1

Transmission model: First, we generate 10^5 MPSK (or MQAM) data symbols α, which are equally likely and have unit (average) energy, that is, $|\alpha|^2 = 1$ for MPSK, and $\mathbf{E}|\alpha^2| = 1$ for MQAM.

Fading channel realizations: In the MCS, we use 10^5 fading and additive white Gaussian noise channel realizations. These many channel realizations are created for source to relay links, that is, $D_1 - R_1$ link and $D_1 - R_2$ link as well as relay to destination links, that is, $R_1 - D_2$ link and $R_2 - D_2$ link. Furthermore, for each channel realization, a data symbol is drawn from the MPSK (MQAM) constellation and is transmitted to the relay node.

Relay selection policy: The selection of the best PA-DAF relay is performed based on PRSP. Based on the source to relays channel statistics, we compute the PA-DAF relay selection probability. This probability is used later in the numerical computation

of various PHY layer performance measures

Relay processing model: Once a noisy version of the data symbol is received by the selected PA-DAF relay, it decodes, and re-encodes. Later, the regenerated signal is amplified by optimum RGF, which is $\mathcal{G}^{\star}(\gamma_1, \gamma_2)$. Note that for each performance parameter, that is, (i) FASER, (ii) FASE, and (iii) FAEE, we have a separate optimization expression to calculate their respective optimum $\mathcal{G}^{\star}(\gamma_1, \gamma_2)$. These optimization expressions are solved using Lagrange multiplier method to get optimum $\mathcal{G}^{\star}(\gamma_1, \gamma_2)$. To calculate $\mathcal{G}^{\star}(\gamma_1, \gamma_2)$, the Lagrange multiplier is set to some initial value and the RGF $\mathcal{G}(\gamma_1, \gamma_2)$ is calculated using Lagrange multiplier method. Once $\mathcal{G}(\gamma_1, \gamma_2)$ is obtained, we use it to verify average power constraint. If the constraint is satisfied with equality, the $\mathcal{G}(\gamma_1, \gamma_2)$ obtained is optimum, otherwise we change the value of Lagrange multiplier till the average power constraint is satisfied with equality. Once the constraint is met, we get $\mathcal{G}^{\star}(\gamma_1, \gamma_2)$. The optimally amplified signal is then transmitted from the selected relay to the destination.

Reception model at the destination: Destination receiver coherently decodes the received symbol using minimum Euclidean distance rule to compute the symbol error. This process is repeated for all the symbols and then averaged to compute the FASER. For the other two scenarios, instantaneous received SNR is computed, and then spectral efficiency and energy efficiency are evaluated.

3.3.2 Numerical Results on Performance Measures

Impact of Relay Transmit power on FASER: All the plots in figure 3.2 show the impact of relay transmit power on FASER. It can be observed from all the plots in figure 3.2 that, as the relay transmit power increases, the FASER decreases.

In figure 3.2a, four cases are plotted which are, i). Varying $\mathcal{G}_{\beta}(\gamma_1, \gamma_2)$ case with PRSP, ii). Fixed $\mathcal{G}_{\beta}(\gamma_1, \gamma_2)$ case with PRSP, iii). Simple DAF case [114] with PRSP, and iv). Simple DAF case with ORSP [56]. Among all the four cases analyzed, our proposed policy that is, varying $\mathcal{G}_{\beta}(\gamma_1, \gamma_2)$ case with PRSP performs best. It can be observed, that the proposed policy achieves the performance gain of 5.5 times with respect to the PRSP with simple DAF relay case and a gain of 11 times is achieved when compared with ORSP with conventional DAF relays.

In figure 3.2b, the plot of FASER versus relay transmit power is shown for the 4-QAM constellation. Here also, the proposed policy outperforms other cases shown in the plot. The proposed policy achieves the gain of 2.1 times in comparison to the system model with simple DAF relays. Furthermore, figure 3.3a shows the plot of higher order modulation scheme, that is, 16 QAM modulation scheme, and the same trend can be observed as for the low order modulation scheme.

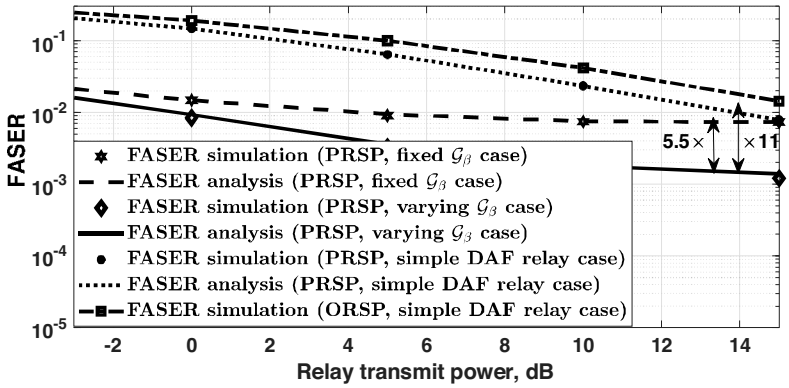

(a) BPSK

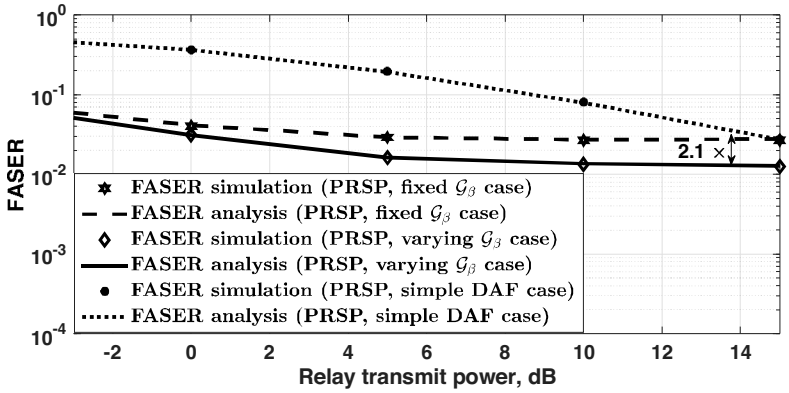

(b) 4-QAM

Figure 3.2: FASER as a function of relay transmit power (P_{th} = 15 dB, mean channel power gain = 1, and $\sigma_n^2 = 1$.).

Figure 3.3b, shows the plot of FASER and it's upper bound with respect to relay transmit power for BPSK and MQAM constellations. It can be observed from the plot, that as the modulation order decreases, the symbol error probability decreases, that is why BPSK performance gain is higher in comparison to the 4-QAM case. Also, the upper bound of both the constellations track their exact FASER well.

Impact of varying P_{th} on FASER: Plots in figure 3.4 shows the impact of varying threshold power P_{th} on FASER. From both the plots it can be observed that as the value of threshold power increases, the RGF increases and the FASER value decreases appreciably.

Impact of varying mean channel power gain on FASER: In figure 3.5, the FASER analysis with varying mean channel power gain is shown. This plot shows the response of the proposed policy when the channel link quality varies. As can be observed from the plot, the proposed policy (in the conditions with low mean channel power gain) outperforms the conventional relaying policies.

Impact of relay transmit power with constant as well as varying P_{th} on FASE: Plots in figure 3.6 show i). the impact of varying relay transmit power and ii). the

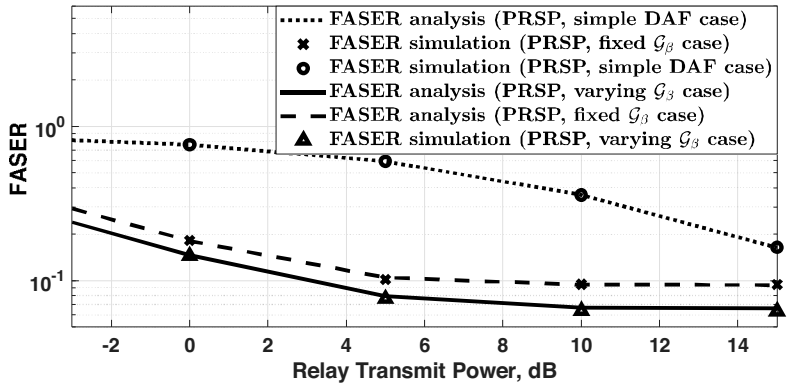

(a) 16-QAM

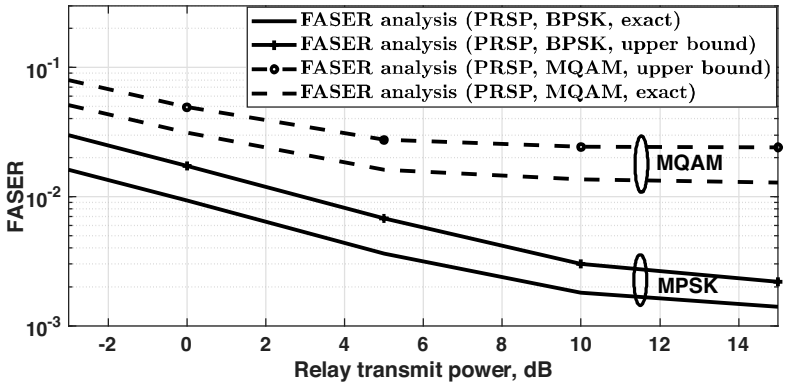

(b) Exact and upper bound plot for BPSK and 4-QAM

Figure 3.3: FASER as a function of relay transmit power for higher order modulation scheme and comparison between exact and upper bound plot for the proposed varying $\mathcal{G}_\beta$ case ($P_{\text{th}} = 15$ dB, mean channel power gain $= 1$, and $\sigma_n^2 = 1$.).

impact of varying threshold power. Among all the cases plotted in figure 3.6a that is, varying $\mathcal{G}$ case, fixed $\mathcal{G}$ case and simple DAF case, the performance of the proposed varying $\mathcal{G}$ case is best. For low relay transmit power also the performance of fading averaged spectral efficiency is good, which is not the case with simple DAF case. It can be observed, from figure 3.6b that as the value of P_{th} increases the performance gain of FASE also increases.

Impact of mean channel power gain on FASE: In figure 3.7, the FASE is plotted against the mean channel power gain. In this plot, the performance of FASE can be observed in different channel conditions. It is essential to analyze the performance of the policy with worst channel conditions, and it can be observed that the proposed policy perform better in adverse channel conditions as well as in good channel conditions in comparison to the conventional relaying policies.

Impact of relay transmit power on FAEE: Plots in figure 3.8 shows the impact of relay transmit power on FAEE. From the first glance on both the plots, it can be observed that as the relay transmit power increases, FAEE decreases. Further, in

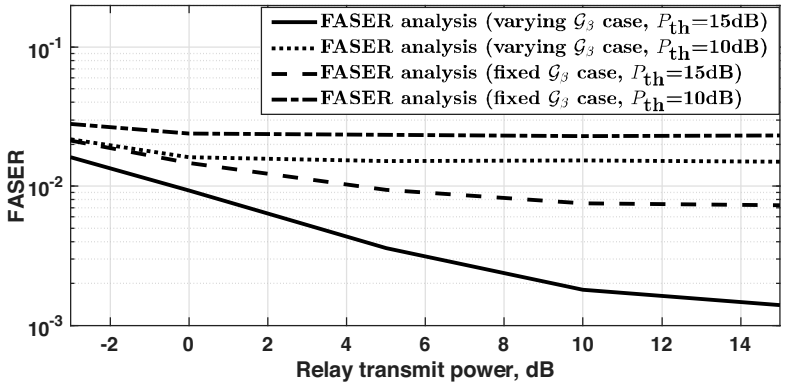

(a) BPSK

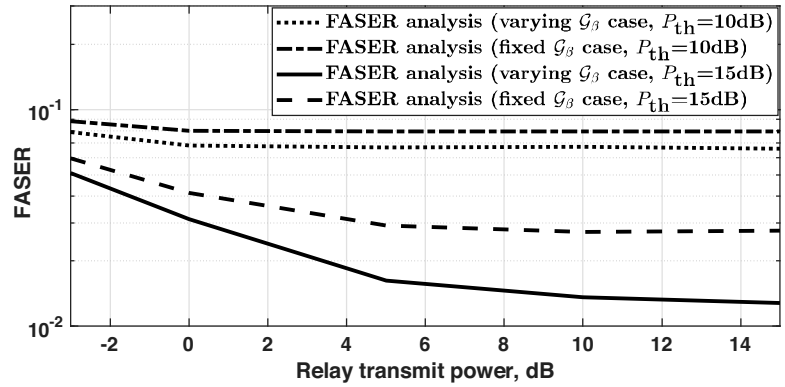

(b) 4-QAM

Figure 3.4: FASER versus relay transmit power for different P_{th} values (Mean channel power gain = 1, and $\sigma_n^2 = 1$.).

figure 3.8a, FAEE is plotted with optimized RGF obtained from FASE case that is, $\mathcal{G}_\eta^*$. Since the $\mathcal{G}_\eta^*$ obtained is minimizing FASE, this will not minimize FAEE. Therefore, it can be observed that for low and medium SNR regimes, the energy efficiency of the proposed policy is less in comparison to conventional policies, since amplification function increases the transmit power of the relay nodes, hence increasing the energy consumption of the relay nodes.

To enhance the performance of the proposed system model in terms of FAEE, a separate maximization problem is defined to enhance FAEE, and the gain obtained from it is $\mathcal{G}_\mathcal{E}^*$. The results for this particular case is shown in figure 3.8b. Here it can be observed that the performance of varying $\mathcal{G}_\mathcal{E}$ case achieves best results in comparison to other relaying cases. This figure also shows the impact of P_{th} on the performance of the proposed policy. As the P_{th} increase, the performance gain also increases.

Impact of mean channel power gain on FAEE: Figure 3.9 shows FAEE with respect to mean channel power gain. In this figure, the response of the proposed policy can be studied for varying channel conditions. It can be observed that as the channel conditions improve, the energy efficiency of the system model increases for all the

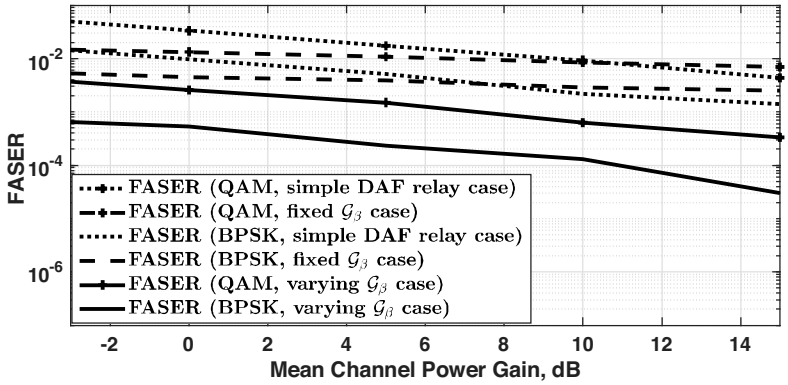

Figure 3.5: FASER as a function of mean channel power gain ($P_r = 5$ dB, $P_{\text{th}} = 15$ dB, and $\sigma_n^2 = 1$.).

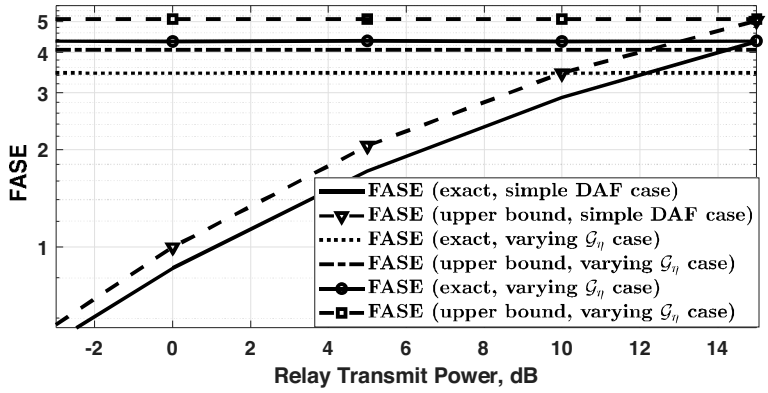

(a) $P_{\text{th}} = 15$ dB

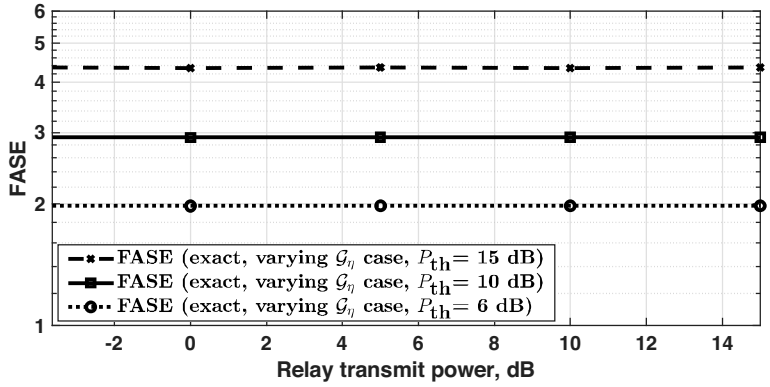

(b) Varying P_{th}

Figure 3.6: FASE as a function of relay transmit power (Mean channel power gain = 1, and $\sigma_n^2 = 1$.).

cases considered. Further, this can also be analyzed from the plot that the proposed policy performs best in comparison to other conventional policy.

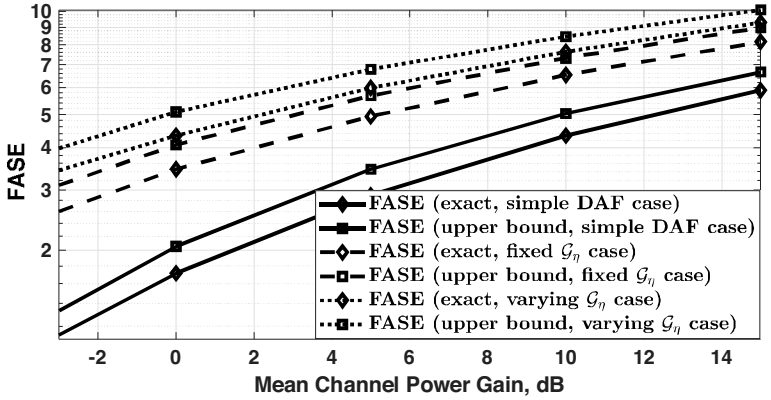

Figure 3.7: FASE as a function of mean channel power gain ($P_r = 5$ dB, $P_{\text{th}} = 15$ dB, and $\sigma_n^2 = 1$.).

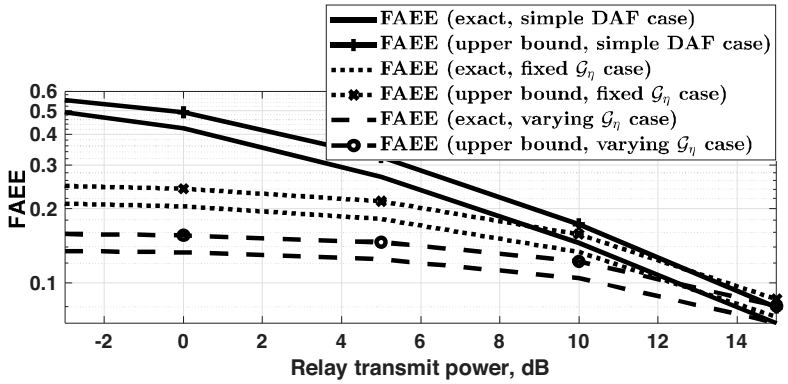

(a) With $\mathcal{G}_\eta^*$

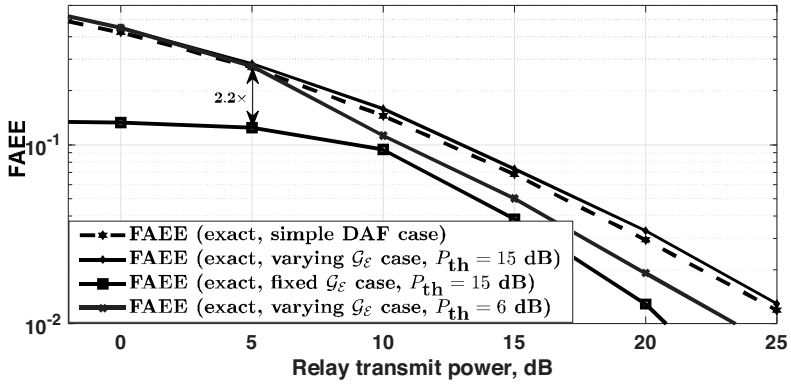

(b) With $\mathcal{G}_\mathcal{E}^*$

Figure 3.8: FAEE as a function of relay transmit power ($P_{\text{th}} = 15$ dB, mean channel power gain = 1, and $\sigma_n^2 = 1$.).

3.4 Summary

In this chapter, we considered a four-node, two-hop cooperative D2D wireless system. We generalized the system model by designing PA-DAF relays. In it, probabilistically selected PA-DAF relay does decoding and jointly adapt its gain and transmit power as

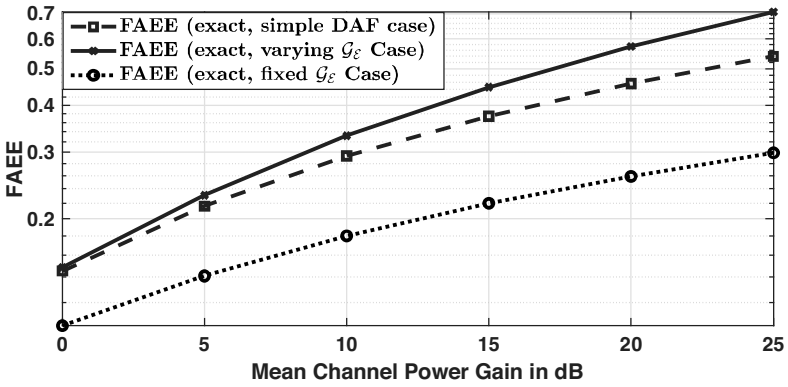

Figure 3.9: FAEE as a function of mean channel power gain ($P_r = 5$ dB, $P_{\text{th}} = 15$ dB, and $\sigma_n^2 = 1$.).

a function of the channel gains to the destination link. For the proposed cooperative D2D system model, we derived FASER optimal, FASE optimal, and FAEE optimal relaying policy. We presented a comprehensive and analytically rich performance analysis of the optimal policies. Specifically, we derived exact analytical expressions for the performance measures and their upper bounds. To gain more insights into the system model, we presented a diversity order analysis. We showed that the diversity order of the proposed FASER optimal policy is one in a scaling regime.

We presented extensive numerical results to validate the derived analytical expressions. Finally, we showed that the proposed optimal relaying policies outperform the benchmark policies. Specifically, we observed that the proposed policy achieves the FASER performance gain of 5.5 times with respect to the PRSP with simple DAF relay case and a gain of 11 times when compared with ORSP with conventional DAF relays at 14 dB for BPSK modulation scheme. We also observed that the proposed PA-DAF policy achieves energy efficiency 2.2 times higher compared to the benchmark fixed gain DAF relaying policy at 5 dB.

Further, since it is quite evident that frequent use of relay nodes in cooperative D2D communication systems can decrease the relay's battery life. Therefore in the next chapter, we will discuss the possible solutions to overcome the battery issues. We will also propose the relay selection policy for the energy-constrained relays to enhance their energy efficiency.